

## Effect of Detector Pose Uncertainty in Localization of Radiation Sources

Doyeon KIM<sup>1,\*</sup>, Hanwool WOO<sup>1</sup>, Yonghoon JI<sup>1</sup>, Yusuke TAMURA<sup>1</sup>,  
Atsushi YAMASHITA<sup>1</sup>, and Hajime ASAMA<sup>1</sup>

<sup>1</sup> *The University of Tokyo, 7-3-1 Hongo, Bunkyo-ku, Tokyo 113-8656, Japan*

### ABSTRACT

For safety and certain removal of the melted down nuclear fuel debris, the localization of radiation sources should be required. In this paper, we propose an approach to estimate the accurate localization of radiation sources by utilizing a gamma-ray CT method with a detector mounted on a mobile robot that has a pose uncertainty. Gamma-ray CT method aggregates measurement data obtained from the detector to localize radiation sources. For applying gamma-ray CT method, detector's position that the measurement data obtained is important. In a simulation experiment, we confirmed the detector's position errors and correlated them with the accuracy of the localization of radiation sources.

### KEYWORDS

*Localization, radiation source, mobile robot, gamma-ray CT*

### ARTICLE INFORMATION

*Article history:*

*Received 7 November 2016*

*Accepted 27 April 2017*

## 1. Introduction

Fukushima Daiichi nuclear power plant, which was damaged by an earthquake and tsunami in 2011, is being decommissioned. To ensure safety during decommissioning, risk management focuses on the removal of radioactive material while preventing exterior leakage [1]. Among the removal tasks, removing the melted-down nuclear fuel debris is the most difficult. Safety and effective removal of the nuclear fuel debris require thorough preparation. The most important step is to localize the fuel debris inside the reactor.

An estimation method by actual unit investigation to localize the fuel debris has been studied. Previous research used a mobile robot in order to investigate inside the primary containment vessel [2]. In reference [3], using imaging technology for the Fukushima Daiichi reactors with cosmic-ray muons to estimate the location of the fuel debris was proposed. Muons have high penetration ability even through thick concrete walls and a reactor pressure vessel. The result of a visualization of the inside of the reactor chamber vessel indicates where most of the fuel debris is located. Nevertheless, the specific location of the fuel debris inside the primary containment chamber, and its properties, are still unknown.

Many studies have been developed for radiation source localization using colocated or distributed detectors. For example, a distributed sensor network deploying many detectors mounted on motor vehicles has performed well in low-level radiation [4–6]. These studies require measurements from at least three detectors connected to each other to observe radiation at a specific time. As the inside area of a nuclear power plant has a complicated and narrow shape, deploying more than two detectors that communicate wirelessly is not realistic.

To estimate the locations of the fuel debris, which is a radiological source, we propose a novel localization scheme based on the gamma-ray CT method [7]. In this research, because of the presence of radiation, a mobile robot equipped with a detector performs an investigation instead of a human. The gamma-ray CT method for localization employs measurement data from several positions surrounding a target object. The gamma-ray CT method in the medical field uses detectors installed with invariable poses to compute a precise estimation of the position information of radiation sources.

\*Corresponding author, E-mail: kim@robot.t.u-tokyo.ac.jp

On the other hand, the pose of the detector utilized in this research has uncertainty because localization of the mobile robot cannot be conducted accurately in general. In this paper, we discuss the effects of the localization method that resulted from uncertainties in the detector pose.

## 2. Localization of radiation sources

### 2.1. Detection of gamma ray

Emitted radiation from sources is measured by a detector consisting of scintillators that absorb radiation. As shown in Fig. 1, collimators [8] are placed on scintillators to constrain the angle of incident radiation in a specific direction. Output data containing coordinates of the scintillator that detects gamma rays and the number of incident gamma rays (i.e., count rate) are obtained from the measurement. Observable incidence angle of the gamma ray is controlled by the collimator as shown in Fig. 1.  $\theta'_{\max}$  is the maximum incident angle of the emitted gamma ray that is able to reach the scintillator unobstructed by the collimators. In this paper, as the size of the scintillator is small ( $0.01 \text{ m} \times 0.01 \text{ m}$ ), we consider that the range of the incident angle of the gamma ray to the scintillator ( $0 \leq \theta' \leq \theta'_{\max}$ ) equals the possible angle of the gamma ray ( $0 \leq \theta \leq \theta_{\max}$ ).

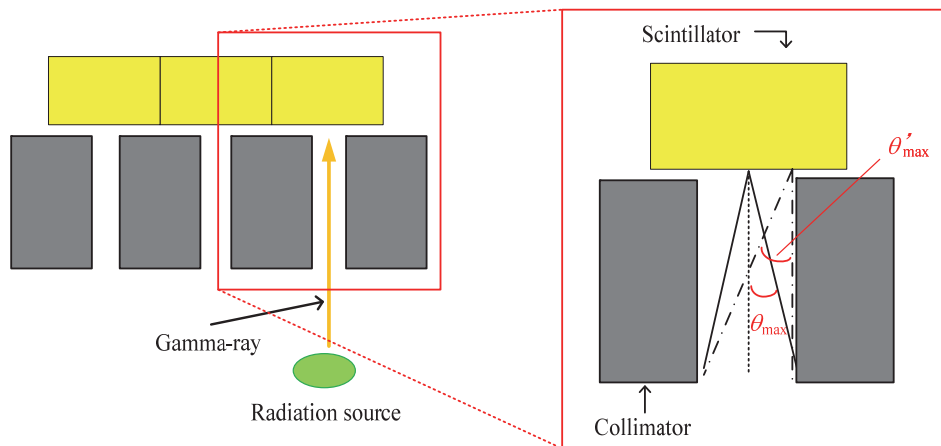


**Fig. 1. Gamma ray detector consisting of collimators and scintillators.**

### 2.2. Measurement using detector mounted on mobile robot

We use a gamma ray detector mounted on a mobile robot to investigate the inside high-radiation environments. Thus, the pose information of the detector is correlated with the pose of the mobile robot, which includes uncertainty. In general, the uncertainty of the robot pose can be represented by a Gaussian distribution [9,10]. The location estimation of radiation sources using measurement data is expected to contain errors.

### 2.3. Localization of source using image reconstruction

This subsection presents a back-projection method to localize sources by combining the measurement data from the detector in a simulation environment. As shown in Fig. 2 (a), measurement data is obtained from a radiation source. If we know the pose of the detector, we can calculate a line that is perpendicular to the detector, as shown in Fig. 2 (b). The lines from the measurement data intersect in the image plane (Fig. 2 (c)). Figure 2 (d) shows the results of a reconstruction based on the back-projection method. The location of the radiation source is estimated at the point of intersection. A detailed explanation of the back-projection method appears in subsection 3.2.

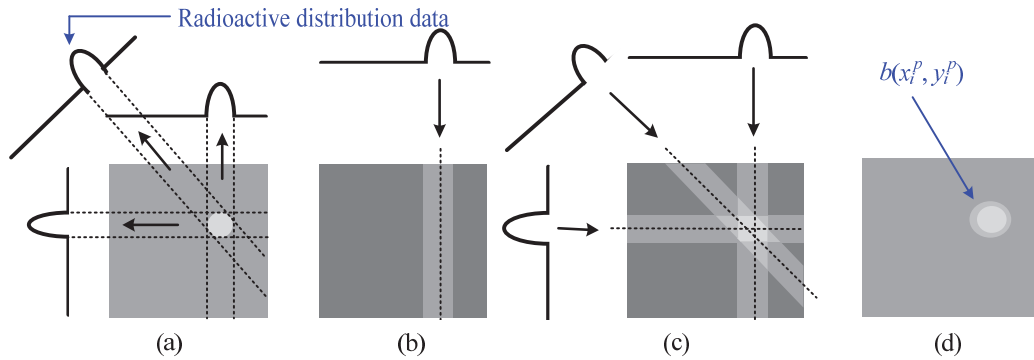


**Fig. 2. Concept of back-projection method: (a) data contains incident radiation emitted source, (b) back-projecting one piece of data obtained from detector to image reconstruction plane, (c) reiterating back-projection with other data, and (d) source localized at overlapped back-projected data.**

### 3. Simulation experiment

#### 3.1. Environment setup

In order to demonstrate the effect of the pose uncertainty on source localization results, a simulation experiment was conducted. In this experiment, we considered that radiation sources are located at the same height as the detector. Thus, we assumed a two-dimensional environment to investigate the validity of performance in the simplest environment given that the proposed methodology for neither 2D nor 3D environment does not widely change. Figure 3 (a) shows the top view of the simulation environment, which includes an 18 m diameter circular carbon steel wall with a thickness of 15 mm. The detector that is mounted on the mobile robot moves in a 6 m × 6 m square path inside the carbon steel wall.

Radiation sources are placed in the middle of an inner circle that has a 4.8 m diameter made of concrete wall as shown in the Fig. 3. (b). In addition, we assume that most of the gamma rays are not scattered by the wall. The experimental environment was built as a simulation using the Geant4 library [11,12], which is a toolkit that simulates radiation, as shown in Fig. 3 (b). The coordinate system of the simulation has its origin at the center of the space. Radiation sources are located at  $S_1$  (1 m, 1 m),  $S_2$  (1 m, -1 m),  $S_3$  (-1 m, -1 m), and  $S_4$  (-1 m, 1 m).

The detector is composed of eight scintillators in a row array, and the size of each scintillator is 0.01 m × 0.01 m. We limited the maximum incident angle to  $\theta_{max} = 1.403^\circ$ . To compute the efficiency, we placed 15 detectors in a row instead of taking several measurements for each movement of the detector. Here, a Gaussian distribution is used to represent the error in the detector’s location (i.e., the pose uncertainty of the mobile robot). The variance of the Gaussian distribution is set as 1.0.

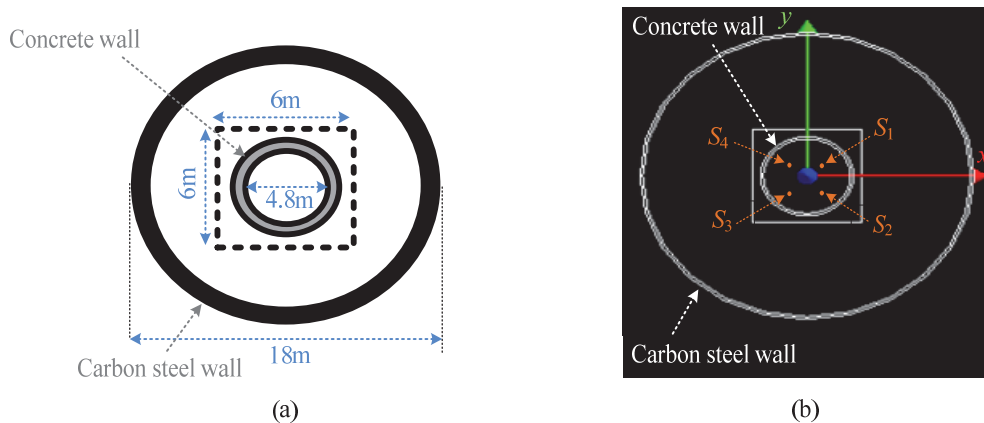


**Fig. 3. Top view of simulation environment: (a) environmental conditions and (b) results of installed environment using Geant4.**

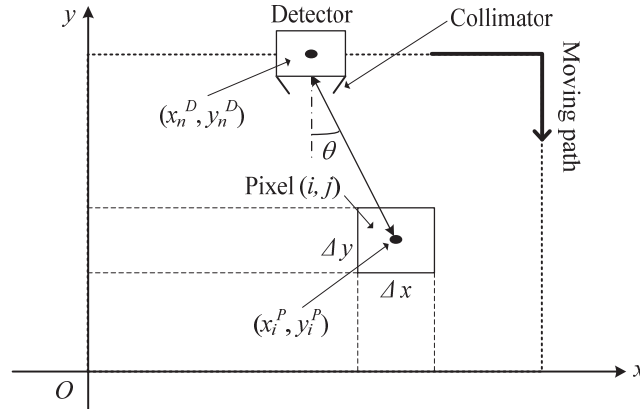


Fig. 4. Back-projection image processing considering the incident angle.

### 3.2. Localization method by back-projection

In this subsection, we describe source localization by a back-projection method using the measurement data obtained in the simulation experiment. The data has a range of incident angle  $\theta$ , as shown in Fig. 4. At the coordinates of the detector position  $(x_n^D, y_n^D)$ , measurement data  $f(x_n^D, y_n^D)$  is obtained by observing the radiation sources. Here,  $n$  denotes the number of observations.

To apply the back-projection method using the observation data, we consider a two-dimensional image reconstruction plane. Each pixel has a size of  $\Delta x = 0.01$  m and  $\Delta y = 0.01$  m. We assume that the detector mounted on the mobile robot moves on its designated path on which there are no obstacles and obtains  $M$  measurement data. Here, the incident angle  $\theta$  between the observation direction and vertical direction to the scintillator is defined, as follows:

$$\theta = \arccos\left(\frac{(y_n^D - y_j^P)}{\sqrt{(x_i^P - x_n^D)^2 + (y_j^P - y_n^D)^2}}\right) \quad (1)$$

Equation (1) converts detector's position  $(x_n^D, y_n^D)$  and image plane pixel information  $(x_i^P, y_j^P)$  which denotes center coordinates of pixel  $(i, j)$  to the incident angle  $\theta$ . Finally, each pixel is assigned aggregated measurement data, which is considered the maximum incident angle ( $\theta \leq \theta_{\max}$ ) as follows:

$$b(x_i^P, y_j^P) = \sum_{n=1}^M f(x_n^D, y_n^D) \quad (2)$$

where function  $b(\cdot)$  means the aggregated measurement data which are accumulated count rates at the coordinates of  $(x_i^P, y_j^P)$  in the reconstruction image plane.

### 3.3. Experimental results

Figure 5 (a) shows a result for the localization of radiation sources without the pose uncertainty of the detector. By contrast, the result shown in Fig. 5 (b) is considered the uncertainty. Images reconstructed by the back-projection method are shown in the upper images in Figs. 5 (a) and (b). Here,  $(x, y)$  indicates a coordinate in the reconstruction image plane and  $z$  is the aggregated measurement data (i.e., count rate). In the image plane, the area where values of  $z$  converge indicates the localized radiation sources. Moreover, the below of the Figs. 5 (a) and (b) respectively show the results for localized radiation sources over 400 count rates and 200 count rates.

As shown at the upper of Fig. 5 (a) and (b), four areas of radiation sources were estimated. For the result without the uncertainty of the pose detector, localized results indicate all positions of radiation sources, including  $\pm 0.02$  m of errors. Likewise, the result that includes the uncertainty of the

detector pose indicates all positions of sources within  $\pm 0.07$  m. As a consequence, the result without the uncertainty of the pose of the detector has a more accurate localization result than that with the uncertainty.

In addition, the converged value of  $z$  from  $S_1$  to  $S_4$  is larger compared with the value of  $z$  from  $S_1'$  to  $S_4'$ . This indicates that the estimated location of the radiation source in Fig. 5 (b) is less reliable than the estimated location of the radiation source in Fig. 5 (a). Because the detector is closer to the location of the radiation source, higher count rates are obtained. Thus, the point with the largest value of  $z$  denotes the location of the radiation source with high possibility. Moreover, in the Fig. 5 (b),  $z$  converges to the single point with noises generated around radiation source position. In conclusion, we confirmed that an uncertainty in the detector pose affects the accuracy of the localization of radiation sources.

The reason for the errors in the result without the uncertainty was the incident angle of the detector, as shown in Figs. 6 (a) and (b). The detector does not consider the maximum incident angle ( $\theta_{\max} = 0$ ). Comparisons were conducted under the same conditions: without considering the maximum incident angle ( $\theta_{\max} = 0$ ) as shown in Fig. 6 (a) and considering the maximum incident angle as shown in Fig. 6 (b). The former case shows the localization results in a single pixel (i.e., a red square in Fig. 6 (a)) at the reconstruction image plane ( $\Delta x$  and  $\Delta y$ ); however, the latter localizes the position of the source for widespread pixels ( $\Delta x'$  and  $\Delta y'$ ).

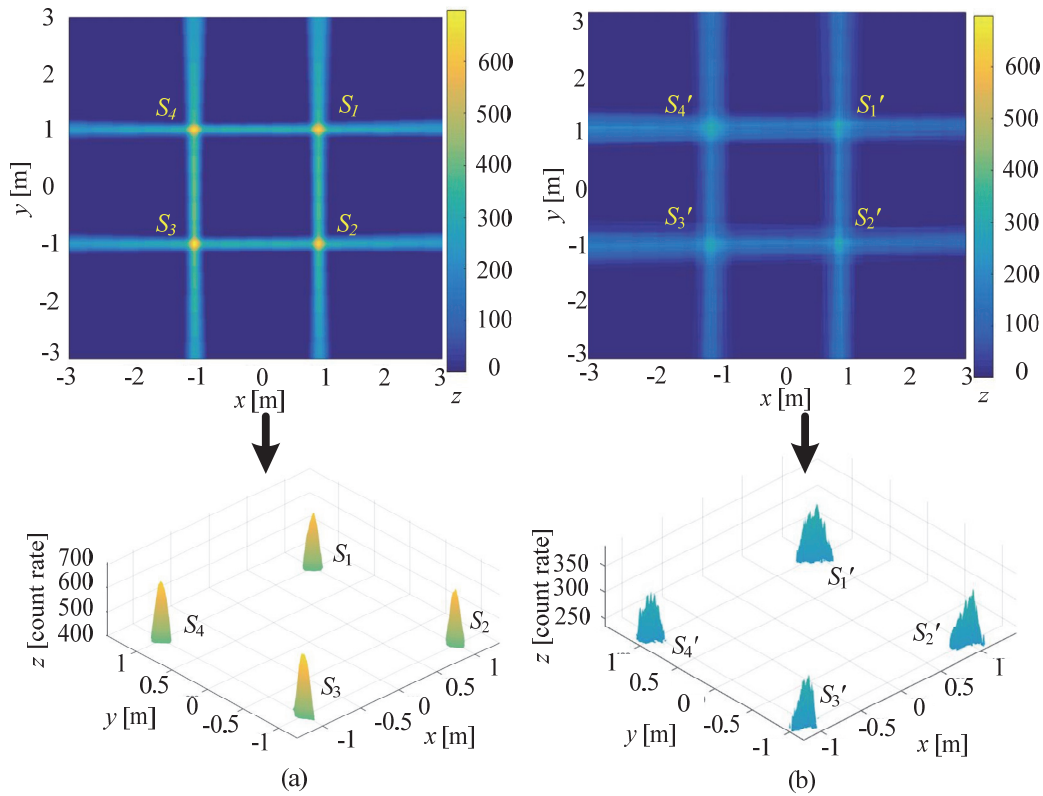


**Fig. 5. Results of localization of radiation sources: (a) results without uncertainty in detector and (b) results with uncertainty in detector.**

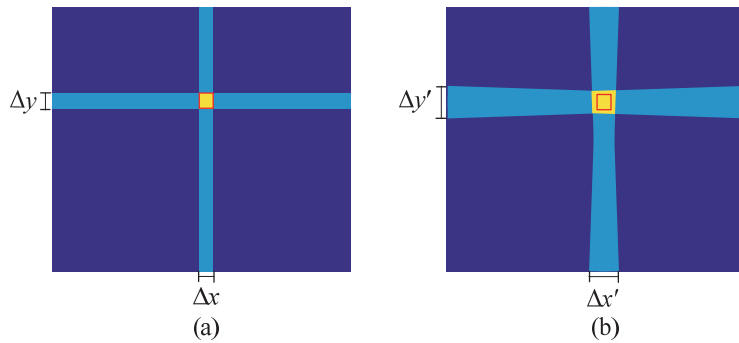


**Fig. 6. Zoomed images of convergence in reconstruction image: (a) converged pixels without considering incident angle range and (b) converged pixels considering incident angle range.**

## 4. Conclusion

This paper proposed a novel localization scheme for radiation sources based on gamma-ray CT using a detector mounted on a mobile robot. We considered an uncertainty in a pose of the detector caused by the mobile robot localization, and demonstrated the results of the localization of radiation sources in a simulation environment. The results indicated that when there is an uncertainty in a detector pose, the estimated localization of radiation sources contains error propagation. Thus, in order to eliminate the errors in the localization results, we plan to apply a simultaneous localization and mapping (SLAM) scheme to estimate the accurate pose of the detector. In addition, a localization method considering a distribution of radiation sources is required, as the fuel debris spread like lava at the Fukushima Daiichi nuclear power plant. Moreover, inside the Fukushima Daiichi nuclear power plant is a complex, narrow area with obstacles, as opposed to the environment that we set up. Therefore, the investigation route for the mobile robot should be discussed further in the future. In addition, even if it is sufficient to conduct the experiment in the two-dimensional environment for verification of the proposed method, we will investigate the validity in more complex environment (i.e., three-dimensional environment) which is more similar to the real world as a future work.

## Acknowledgement

Part of this study is the result of “HRD for Fukushima Daiichi Decommissioning Based on Robotics and Nuclide Analysis” carried out under the Center of World Intelligence Project for Nuclear S&T and Human Resource Development by the Ministry of Education, Culture, Sports and Technology of Japan.

## References

- [1] Nuclear Emergency Response Headquarters: “Mid-and-Long-Term Roadmap Towards the Decommissioning of TEPCO’s Fukushima Daiichi Nuclear Power Station Units 1–4”, Ministry of Economy, Trade and Industry Press Release Archive (2015) [http://www.meti.go.jp/english/press/2013/pdf/0627\\_01.pdf](http://www.meti.go.jp/english/press/2013/pdf/0627_01.pdf) (Accessed October 14, 2016).
- [2] Tokyo Electric Power Corporation: “Development of a Technology to Investigate Inside the Reactor Primary Containment Vessel (PCV)”, Tokyo Electric Power Co. Press Release Archive (2012-2015) [http://www.tepco.co.jp/en/nu/fukushima-np/handouts/2015/images/handouts\\_150430\\_04-e.pdf](http://www.tepco.co.jp/en/nu/fukushima-np/handouts/2015/images/handouts_150430_04-e.pdf) (Accessed October 14, 2016)
- [3] H. Miyadera, K. N. Borozdin, S. J. Greene, Z. Lukic, K. Masuda, E. C. Milner, C. L. Morris, and J. O. Perry: “Imaging Fukushima Daiichi Reactors with Muons”, *AIP Advances*, Vol. 3, No. 3, pp. 052133, 2013.
- [4] N. S. V. Rao, M. Shankar, J. C. Chin, D. K. Y. Yau, S. Srivathsan, S. S. Iyengar, Y. Yang, and J. C. Hou: “Identification of Low-Level Point Radiation Sources Using a Sensor Network”, *Proceedings of ACM/IEEE International Conference on Information Processing in Sensor Networks (IPSN)*, pp. 493–504, 2008.



- [5] R. J. Nemzek, J. S. Dreicer, D. C. Torney, and T. T. Warnock: “Distributed Sensor Networks for Detection of Mobile Radioactive Sources”, *IEEE Transactions on Nuclear Science*, Vol. 51, No. 4, pp. 1693–1700, 2004.
- [6] J. Chin, D. Yau, N. Rao, Y. Yang, C. Ma, and M. Shankar: “Accurate Localization of Low-level Radioactive Source Under Noise and Measurement Errors”, *Proceedings of the 6<sup>th</sup> ACM Conference on Embedded Network Sensor Systems*, pp. 183–196, 2008.
- [7] H. Turbell: “Cone-Beam Reconstruction Using Filtered Backprojection”, Ph. D. Dissertation, Linkoping University, Sweden, 2001.
- [8] C. J. Thompson: “The Effect of Collimation on Scatter Fraction in Multi-slice PET”, *IEEE Transactions on Nuclear Science*, Vol. 35, No. 1, pp. 598-602, 1988.
- [9] S. Thrun, W. Burgard, and D. Fox: “Probabilistic Robotics”, MIT Press, 2005.
- [10] H. Durrant-Whyte and T. Bailey: “Simultaneous Localization and Mapping: Part I”, *IEEE Robotics & Automation Magazine*, Vol. 13, No. 2, pp. 99–110, 2006.
- [11] S. Agostinelli, et al.: “GEANT4-A Simulation Toolkit”, *Nuclear Instruments and Methods in Physics Research Section A: Accelerators, Spectrometers, Detectors and Associated Equipment*, Vol. 506, No. 3, pp. 250–303, 2003.
- [12] J. Allison, et al.: “Geant4 Developments and Applications”, *IEEE Transactions on Nuclear Science*, Vol. 53, No. 1, pp. 270–278, 2006.